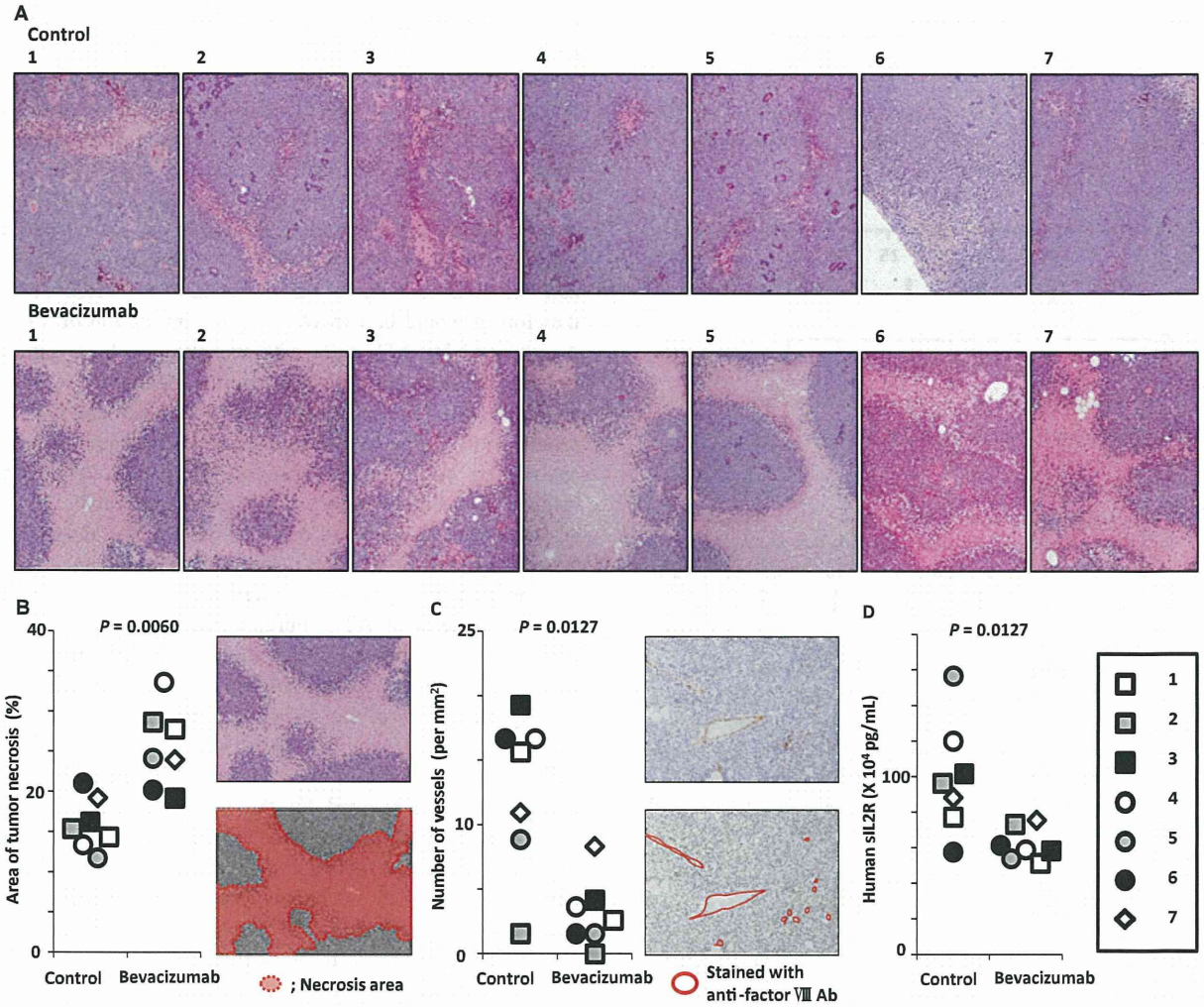

Figure 4 Bevacizumab therapy has significant therapeutic efficacy in the ATL cell-bearing NOG mouse model. (A) Macroscopic photomicrographs with hematoxylin and eosin staining of mice given saline (control) (upper panels) or bevacizumab (lower panels). (B) Area of tumor necrosis (%) of each ATL cell-bearing NOG mouse. The bevacizumab-treated mice had significantly greater tumor necrosis than control mice (left panel). An example of a calculation for tumor necrosis area (%) by means of Image J software is shown (right panels). (C) Numbers of vessels (/mm^2) of each ATL cell-bearing NOG mouse. The bevacizumab recipients had significantly fewer vessels than controls (left panel). An example of such a calculation by means of Image J software is shown (right panels). (D) Serum sIL2R concentrations of each ATL cell-bearing NOG mouse. The bevacizumab recipients had significantly lower levels of sIL2R than controls.

the tumor burden of the human CD25-expressing ATL (26). Treatment with bevacizumab showed significantly greater therapeutic efficacy as demonstrated by sIL2R concentrations in S-YU cell-bearing NOG mice (617.9, 588.5, 513.2–755.7 $\times$ 10^3 pg/mL), compared to controls (996.6, 963.4, 575.7–1565.0 $\times$ 10^3 pg/mL, P = 0.0127) (Fig. 4D). Although bevacizumab monotherapy showed significant therapeutic efficacy as demonstrated by the percentage of tumor necrosis, vascular number in the tumor tissues, and sIL2R concentrations in sera (Fig. 4), it did not confer any survival advantage to the NOG/S-YU mice (Fig. 5A). No toxicity attributable to bevacizumab injections was observed in any of the mice in this setting.

Therapeutic efficacy of bevacizumab plus CHOP compared to CHOP alone in S-YU cell-bearing NOG mice

The bevacizumab plus CHOP group did have a significant prolongation of survival compared with CHOP alone (P = 0.046). The median survival time of bevacizumab plus CHOP and CHOP alone was 38 and 34 d, respectively.

Discussion

In this study, we have demonstrated that bevacizumab possesses significant therapeutic efficacy in an ATL mouse model in which the tumor cells from a patient survive and

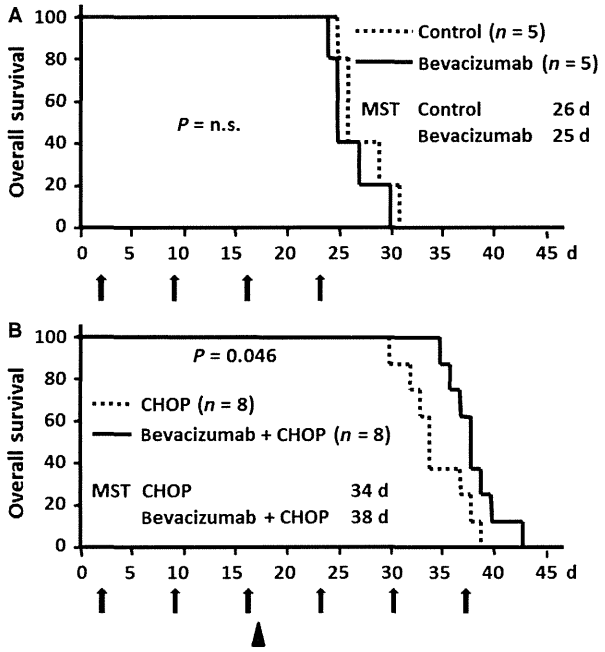

Figure 5 Survival analysis of ATL cell-bearing NOG mice treated with bevacizumab (A) Kaplan–Meier survival curves of ATL cell-bearing NOG mice treated with bevacizumab or saline. Arrows, bevacizumab or control (saline) injections. Each group consists of five mice. The difference between the bevacizumab and control groups is not significant. (B) Kaplan–Meier survival curves of ATL cell-bearing NOG mice treated with bevacizumab + CHOP, or CHOP alone. Arrows, bevacizumab or control (saline) injections. Arrow head, CHOP injection. Each group consists of eight mice. The difference between the bevacizumab + CHOP and CHOP alone is statistically significant.

proliferate in a murine microenvironment-dependent manner. The present finding revealed the importance of angiogenesis for the pathogenesis of VEGF-expressing ATL.

NOG mice have severe, multiple immune defects, such that human immune cells engrafted into them retain essentially the same functions as in humans (27, 28). While it has been reported that S-YU cells can be serially transplanted into SCID mice as recipients, the present study demonstrated that S-YU cells could also be serially transplanted into NOG mice. This was not unexpected given the even more severe immune dysfunction of NOG mice compared to SCID mice. This may also explain why the ATL tumor masses were much larger in NOG than in SCID mice.

In this study, most primary ATL cases (22/23), and all of the established cell lines tested (7/7), were positive for VEGF-A. These results are consistent with data from other investigators (16, 18, 19). Thus, the VEGF-A produced by ATL cells is likely to play an important role in the pathogenesis of ATL. On the other hand, *VEGF-R1 mRNA* expression was only seen in two of the seven ATL and HTLV-1-immortalized lines, and *VEGF–R2* in none of them. VEGF-R1 protein expression by primary ATL tumor cells was only seen in one of nine patients, and VEGF-R2 in none. In B-cell lymphomas, an earlier study reported that tumor cell growth was promoted in an autocrine fashion via VEGF-A/VEGF-R1 or VEGF-A/VEGF-R2 interactions (29). However, the present analysis of VEGF-R1/R2 expression in ATL, and the results of *in vitro* proliferation assays, did not support the existence of such an autocrine loop in ATL.

Because S-YU cells can only be maintained by serial transplantation in immunodeficient mice, but not by *in vitro* culture (30), the microenvironment is likely to be indispensable for their survival. S-YU are positive for VEGF-A, and therefore it would be expected that the interaction of VEGF-A produced by ATL cells with receptors on host (murine) endothelial cells should play an important role in tumor angiogenesis. This would lead to tumor cell survival and proliferation supported by transport of sufficient nutrients and oxygen in the mouse. Therefore, the present ATL model using S-YU should better reflect the human ATL *in vivo* environment, compared to other mouse models using established ATL cell lines, or HTLV-1-immortalized lines. Thus, this model should provide a powerful tool for understanding the pathogenesis of ATL. Furthermore, it should be useful not only for evaluating novel cytotoxic anti-ATL agents, but also provide a more appropriate *in vivo* model to test antitumor agents targeting the microenvironment, including bevacizumab.

The effect observed in mice receiving bevacizumab monotherapy, as demonstrated by the increased tumor necrosis area and reduced vasculature in the tumor tissue, was expected, given the conventional antitumor mechanism of bevacizumab, which neutralizes the human VEGF-A produced by the tumor cells, but not murine VEGF-A (31). It then inhibits the growth of new blood vessels and thus starves tumor cells of necessary nutrients and oxygen (32). This should lead to a reduced tumor burden, as indicated by the sIL2R concentrations measured. Although bevacizumab monotherapy did show this anti-angiogenesis effect, it did not lead to survival prolongation in this study. This finding is consistent with the clinical observations in many types of cancer such as colorectal cancer, non-small-cell lung cancer, renal cell carcinoma, and ovarian cancer. On the other hand, combination treatment with bevacizumab and CHOP did prolong survival compared to CHOP alone. Nonetheless, the extent of this prolongation was not marked, which is also consistent with clinical observations in many types of cancer where bevacizumab is of limited benefit and then only when combined with chemotherapy. This study suggested that the tumor cell 'starvation effect' alone mediated by bevacizumab does not result in prolonged survival. It has been reported that VEGF-targeted therapy can 'normalize' the tumor vascular network and that this can lead to a more uniform blood flow, with subsequent increased delivery of chemotherapeutic agents (33, 34). This normalization by bevacizumab is a possible explanation for the prolonged survival in the present combination setting.

The present study demonstrated the importance of angiogenesis for the pathogenesis of ATL and the potential efficacy of blocking this in at least a subgroup of patients with ATL. In recent clinical cancer therapy experience, the epidermal growth factor receptor (EGFR) tyrosine kinase inhibitor, gefitinib, failed to yield significantly improved overall survival in patients with refractory NSCLC, but did show therapeutic benefit in a subgroup of patients with mutated EGFR (35). In the case of mAb targeting the EGFR, both panitumumab and cetuximab also yield clinical benefits only in a subgroup of colorectal cancer patients with wild-type *KRAS* and BRAF (36). These findings indicate that we should develop novel treatment strategies based on tumor biology, and not on tumor category. Therefore, as a next step, further investigations are warranted to determine which subgroups of patients with ATL will benefit from bevacizumab therapy (37). In other words, we should face the challenge of developing robust biomarkers that can guide selection of those patients with ATL for whom bevacizumab therapy will be most beneficial. In addition, several promising new agents for treating ATL are currently being developed (1, 38–40). Investigations of combinations of bevacizumab with these novel agents are also warranted.

In conclusion, to the best of our knowledge this is the first report to evaluate the efficacy of bevacizumab for ATL in a tumor microenvironment-dependent animal model. Bevacizumab therapy combined with chemotherapy could be a potential treatment strategy for that subgroup of patients with ATL probably depending to a large extent on angiogenesis via VEGF for tumor survival and proliferation.

Acknowledgements

We thank Ms Chiori Fukuyama for her excellent technical assistance and Ms. Naomi Ochiai for her excellent secretarial assistance.

Funding

This study was supported by Grants-in-Aid for Scientific Research (B) (No. 25290058, T. Ishida), and Scientific Support Programs for Cancer Research (No. 221S0001, T. Ishida) from the Ministry of Education, Culture, Sports, Science and Technology of Japan, Grants-in-Aid for National Cancer Center Research and Development Fund (No. 21-6-3, T. Ishida), and H23-Third Term Comprehensive Control Research for Cancer-general-011, T. Ishida, from the Ministry of Health, Labour and Welfare, Japan.

Authorship contributions

Mori F, Ishida T, Asahi I, and Ueda R designed the research. Mori F, Ishida T, Asahi I, Sato F, Masaki A, Narita T, Suzuki S, Yamada T, and Takino H performed the research. Hishizawa M, Imada K, Takaori-Kondo A contributed to establishing the ATL mouse model. All the authors analyzed the data and wrote the article.

Conflict of interest

Nagoya City University Graduate School of Medical Sciences has received research funding for Takashi Ishida, Shigeru Kusumoto, and Shinsuke Iida from Chugai Pharmaceutical Co., Ltd. The other authors have no financial conflicts of interest related with this study.

References

1. Ishida T, Ueda R. Antibody therapy for adult T-cell leukemia-lymphoma. *Int J Hematol* 2011;**94**:443–52.
2. Matsuoka M, Jeang KT. Human T-cell leukaemia virus type 1 (HTLV-1) infectivity and cellular transformation. *Nat Rev Cancer* 2007;**7**:270–80.
3. Shimoyama M. Diagnostic criteria and classification of clinical subtypes of adult T-cell leukaemia-lymphoma. A report from the Lymphoma Study Group (1984–87). *Br J Haematol* 1991;**79**:428–37.
4. Uchiyama T, Yodoi J, Sagawa K, Takatsuki K, Uchino H. Adult T-cell leukemia: clinical and hematologic features of 16 cases. *Blood* 1977;**50**:481–92.
5. Ishida T, Hishizawa M, Kato K, *et al.* Allogeneic hematopoietic stem cell transplantation for adult T-cell leukemia-lymphoma with special emphasis on preconditioning regimen: a nationwide retrospective study. *Blood* 2012;**120**:1734–41.
6. Utsunomiya A, Miyazaki Y, Takatsuka Y, *et al.* Improved outcome of adult T cell leukemia/lymphoma with allogeneic hematopoietic stem cell transplantation. *Bone Marrow Transplant* 2001;**27**:15–20.
7. Carmeliet P, Jain RK. Molecular mechanisms and clinical applications of angiogenesis. *Nature* 2011;**473**:298–307.
8. Burger RA, Brady MF, Bookman MA, *et al.* Incorporation of bevacizumab in the primary treatment of ovarian cancer. *N Engl J Med* 2011;**365**:2473–83.
9. Escudier B, Pluzanska A, Koralewski P, *et al.* Bevacizumab plus interferon alfa-2a for treatment of metastatic renal cell carcinoma: a randomised, double-blind phase III trial. *Lancet* 2007;**370**:2103–11.
10. Escudier B, Bellmunt J, Négrier S, Bajetta E, Melichar B, Bracarda S, Ravaud A, Golding S, Jethwa S, Sneller V. Phase III trial of bevacizumab plus interferon alfa-2a in patients with metastatic renal cell carcinoma (AVOREN): final analysis of overall survival. *J Clin Oncol* 2010;**28**:2144–50.
11. Hurwitz H, Fehrenbacher L, Novotny W, *et al.* Bevacizumab plus irinotecan, fluorouracil, and leucovorin for metastatic colorectal cancer. *N Engl J Med* 2004;**350**:2335–42.
12. Perren TJ, Swart AM, Pfisterer J, *et al.* A phase 3 trial of bevacizumab in ovarian cancer. *N Engl J Med* 2011;**365**:2484–96.

13. Sandler A, Gray R, Perry MC, Brahmer J, Schiller JH, Dowlati A, Lilenbaum R, Johnson DH. Paclitaxel-carboplatin alone or with bevacizumab for non-small-cell lung cancer. *N Engl J Med* 2006;**355**:2542–50.
14. Yang JC, Haworth L, Sherry RM, Hwu P, Schwartzentruber DJ, Topalian SL, Steinberg SM, Chen HX, Rosenberg SA. A randomized trial of bevacizumab, an anti-vascular endothelial growth factor antibody, for metastatic renal cancer. *N Engl J Med* 2003;**349**:427–34.
15. Kreisl TN, Kim L, Moore K, *et al.* Phase II trial of single-agent bevacizumab followed by bevacizumab plus irinotecan at tumor progression in recurrent glioblastoma. *J Clin Oncol* 2009;**27**:740–5.
16. Bazarbachi A, Abou Merhi R, Gessain A, *et al.* Human T-cell lymphotropic virus type I-infected cells extravasate through the endothelial barrier by a local angiogenesis-like mechanism. *Cancer Res* 2004;**64**:2039–46.
17. El-Sabban ME, Merhi RA, Haidar HA, Arnulf B, Khoury H, Basbous J, Nijmeh J, de Thé H, Hermine O, Bazarbachi A. Human T-cell lymphotropic virus type 1-transformed cells induce angiogenesis and establish functional gap junctions with endothelial cells. *Blood* 2002;**99**:3383–9.
18. Hayashibara T, Yamada Y, Miyanishi T, Mori H, Joh T, Maeda T, Mori N, Maita T, Kamihira S, Tomonaga M. Vascular endothelial growth factor and cellular chemotaxis: a possible autocrine pathway in adult T-cell leukemia cell invasion. *Clin Cancer Res* 2001;**7**:2719–26.
19. Watters KM, Dean J, Gautier V, Hall WW, Sheehy N. Tax 1-independent induction of vascular endothelial growth factor in adult T-cell leukemia caused by human T-cell leukemia virus type 1. *J Virol* 2010;**84**:5222–8.
20. Ito M, Kobayashi K, Nakahata T. NOD/Shi-scid IL2rgnull (NOG) mice more appropriate for humanized mouse models. *Curr Top Microbiol Immunol* 2008;**324**:53–76.
21. Abramoff MD, Magelhaes PJ, Ram SJ. Image Processing with ImageJ. *Biophotonics Int* 2004;**11**:36–42.
22. Imada K, Takaori-Kondo A, Sawada H, Imura A, Kawamata S, Okuma M, Uchiyama T. Serial transplantation of adult T cell leukemia cells into severe combined immunodeficient mice. *Jpn J Cancer Res* 1996;**87**:887–92.
23. Suzuki S, Masaki A, Ishida T, *et al.* Tax is a potential molecular target for immunotherapy of adult T-cell leukemia/lymphoma. *Cancer Sci* 2012;**103**:1764–73.
24. Mori F, Ishida T, Ito A, *et al.* Potent antitumor effects of bevacizumab in a microenvironment-dependent human lymphoma mouse model. *Blood Cancer J* 2012;**2**:e67.
25. Mohammad RM, Wall NR, Dutcher JA, Al-Katib AM. The addition of bryostatin 1 to cyclophosphamide, doxorubicin, vincristine, and prednisone (CHOP) chemotherapy improves response in a CHOP-resistant human diffuse large cell lymphoma xenograft model. *Clin Cancer Res* 2000;**6**:4950–6.
26. Motoi T, Uchiyama T, Uchino H, Ueda R, Araki K. Serum soluble interleukin-2 receptor levels in patients with adult T-cell leukemia and human T-cell leukemia/lymphoma virus type-I seropositive healthy carriers. *Jpn J Cancer Res* 1988;**79**:593–9.
27. Ito A, Ishida T, Utsunomiya A, *et al.* Defucosylated anti-CCR4 monoclonal antibody exerts potent ADCC against primary ATLL cells mediated by autologous human immune cells in NOD/Shi-scid, IL-2R gamma(null) mice *in vivo*. *J Immunol* 2009;**183**:4782–91.
28. Masaki A, Ishida T, Suzuki S, *et al.* Autologous Tax-Specific CTL therapy in a primary adult T cell leukemia/lymphoma cell-bearing NOD/Shi-scid, IL-2Rγnull mouse model. *J Immunol* 2013;**191**:135–44.
29. Wang ES, Teruya-Feldstein J, Wu Y, Zhu Z, Hicklin DJ, Moore MA. Targeting autocrine and paracrine VEGF receptor pathways inhibits human lymphoma xenografts *in vivo*. *Blood* 2004;**104**:2893–902.
30. Koga H, Imada K, Ueda M, Hishizawa M, Uchiyama T. Identification of differentially expressed molecules in adult T-cell leukemia cells proliferating *in vivo*. *Cancer Sci* 2004;**95**:411–7.
31. Yu L, Wu X, Cheng Z, Lee CV, LeCouter J, Campa C, Fuh G, Lowman H, Ferrara N. Interaction between bevacizumab and murine VEGF-A: a reassessment. *Invest Ophthalmol Vis Sci* 2008;**49**:522–7.
32. Ellis LM, Hicklin DJ. VEGF-targeted therapy: mechanisms of anti-tumour activity. *Nat Rev Cancer* 2008;**8**:579–91.
33. Carmeliet P, Jain RK. Principles and mechanisms of vessel normalization for cancer and other angiogenic diseases. *Nat Rev Drug Discov* 2011;**10**:417–27.
34. Jain RK. Normalization of tumor vasculature: an emerging concept in antiangiogenic therapy. *Science* 2005;**307**:58–62.
35. Maemondo M, Inoue A, Kobayashi K, *et al.* Gefitinib or chemotherapy for non-small-cell lung cancer with mutated EGFR. *N Engl J Med* 2010;**362**:2380–8.
36. Bardelli A, Siena S. Molecular mechanisms of resistance to cetuximab and panitumumab in colorectal cancer. *J Clin Oncol* 2010;**28**:1254–61.
37. Lambrechts D, Lenz HJ, de Haas S, Carmeliet P, Scherer SJ. Markers of response for the antiangiogenic agent bevacizumab. *J Clin Oncol* 2013;**31**:1219–30.
38. Ishida T, Joh T, Uike N, *et al.* Defucosylated anti-CCR4 monoclonal antibody (KW-0761) for relapsed adult T-cell leukemia-lymphoma: a multicenter phase II study. *J Clin Oncol* 2012;**30**:837–42.
39. Tanosaki R, Tobinai K. Adult T-cell leukemia-lymphoma: current treatment strategies and novel immunological approaches. *Expert Rev Hematol* 2010;**3**:743–53.
40. Marçais A, Suarez F, Sibon D, Frenzel L, Hermine O, Bazarbachi A. Therapeutic options for adult T-cell leukemia/lymphoma. *Curr Oncol Rep* 2013;**15**:457–64.

Human CD1c$^+$ Myeloid Dendritic Cells Acquire a High Level of Retinoic Acid–Producing Capacity in Response to Vitamin D_3

Takayuki Sato,*,† Toshio Kitawaki,* Haruyuki Fujita,* Makoto Iwata,†,‡ Tomonori Iyoda,†,§ Kayo Inaba,†,§ Toshiaki Ohteki,†,¶ Suguru Hasegawa,‖ Kenji Kawada,‖ Yoshiharu Sakai,‖ Hiroki Ikeuchi,# Hiroshi Nakase,** Akira Niwa,††,‡‡ Akifumi Takaori-Kondo,* and Norimitsu Kadowaki*,†

All-*trans*-retinoic acid (RA) plays a critical role in maintaining immune homeostasis. Mouse intestinal CD103$^+$ dendritic cells (DCs) produce a high level of RA by highly expressing retinal dehydrogenase (RALDH)2, an enzyme that converts retinal to RA, and induce gut-homing T cells. However, it has not been identified which subset of human DCs produce a high level of RA. In this study, we show that CD1c$^+$ blood myeloid DCs (mDCs) but not CD141^{high} mDCs or plasmacytoid DCs exhibited a high level of RALDH2 mRNA and aldehyde dehydrogenase (ALDH) activity in an RA- and p38-dependent manner when stimulated with 1α,25-dihydroxyvitamin D_3 (VD_3) in the presence of GM-CSF. The ALDH activity was abrogated by TLR ligands or TNF. CD103$^-$ rather than CD103$^+$ human mesenteric lymph node mDCs gained ALDH activity in response to VD_3. Furthermore, unlike in humans, mouse conventional DCs in the spleen and mesenteric lymph nodes gained ALDH activity in response to GM-CSF alone. RALDH2^{high} CD1c$^+$ mDCs stimulated naive CD4$^+$ T cells to express gut-homing molecules and to produce Th2 cytokines in an RA-dependent manner. This study suggests that CD1c$^+$ mDCs are a major human DC subset that produces RA in response to VD_3 in the steady state. The "vitamin D – CD1c$^+$ mDC – RA" axis may constitute an important immune component for maintaining tissue homeostasis in humans. *The Journal of Immunology*, **2013, 191: 3152–3160.**

Dendritic cells (DCs) play a pivotal role in controlling immune responses in terms of their magnitude and quality, such as immunity versus tolerance, depending on the tissue milieu. This eventually leads to maintaining immune homeostasis by eliminating pathogens and by avoiding harmful inflammation. Recent studies using mice revealed the importance of all-*trans*-retinoic acid (hereafter referred to as RA) derived from DCs in maintaining immune homeostasis in the intestine (1) and possibly in other organs (2). It has been shown that CD103$^+$ DCs in lamina propria and mesenteric lymph nodes (MLNs) produce RA and thus to promote the generation of gut-homing regulatory T (Treg) cells (3). GM-CSF (4) and RA (4–8) are pivotal factors to induce mouse DCs to express retinal dehydrogenase (RALDH)2, which is encoded by the aldehyde dehydrogenase 1 family, member A2 (*ALDH1A2*) gene and converts retinal to RA. IL-4 (4, 9) and TLR ligands (2, 4, 5, 10–12) augment the expression of RALDH2. These studies have presented a model that appropriately stimulated CD103$^+$ DCs in gut-associated tissues produce RA and thus induce gut-homing Treg cells, resulting in maintaining immune homeostasis in the intestine in mice. Surprisingly, however, human DCs that express a high level of RALDH have not been identified.

Human DC subsets in blood and lymphoid tissues are composed of myeloid DCs (mDCs) and plasmacytoid DCs (pDCs) (13). mDCs are further subdivided into CD141 (BDCA-3)^{high} mDCs and CD1c (BDCA-1)$^+$ mDCs, and the former corresponds to mouse CD8$^+$ CD11b$^-$ conventional DCs (cDCs) in lymphoid tissues (14–16) and CD103$^+$ cDCs in nonlymphoid tissues (17) that efficiently cross-present Ags. In contrast, distinctive functions of the latter, which is likely equivalent to mouse CD8$^-$CD11b$^+$ cDCs (18), have been elusive. In addition, monocytes and CD34$^+$ hematopoietic progenitors can differentiate into DCs in the presence of appropriate cytokine mixtures. However, it remains unclear which DCs in situ correspond to DCs induced in vitro from monocytes or CD34$^+$ progenitors. Therefore, it is important to obtain data using DCs isolated from blood and tissues to gain an insight into physiological and clinical relevance of basic researches on human DCs.

*Department of Hematology and Oncology, Graduate School of Medicine, Kyoto University, Kyoto 606-8507, Japan; †Japan Science and Technology Agency, Core Research for Evolutional Science and Technology, Tokyo 102-0076, Japan; ‡Laboratory of Immunology, Kagawa School of Pharmaceutical Sciences, Tokushima Bunri University, Kagawa 769-2193, Japan; §Division of Systemic Life Science, Department of Animal Development and Physiology, Laboratory of Immunology, Graduate School of Biostudies, Kyoto University, Kyoto 606-8501, Japan; ¶Department of Biodefense Research, Medical Research Institute, Tokyo Medical and Dental University, Tokyo 101-0062, Japan; ‖Department of Surgery, Graduate School of Medicine, Kyoto University, Kyoto 606-8507, Japan; #Department of Surgery, Hyogo College of Medicine, Hyogo 663-8501, Japan; **Department of Gastroenterology and Hepatology, Graduate School of Medicine, Kyoto University, Kyoto 606-8507, Japan; ††Department of Pediatrics, Graduate School of Medicine, Kyoto University, Kyoto 606-8507, Japan; and ‡‡Department of Clinical Application, Center for iPS Cell Research and Application, Kyoto University, Kyoto 606-8507, Japan

Received for publication December 26, 2012. Accepted for publication July 16, 2013.

This work was supported by research funding from the Japan Science and Technology Agency, Core Research for Evolutional Science and Technology (to N.K.).

Address correspondence and reprint requests to Dr. Norimitsu Kadowaki, Department of Hematology and Oncology, Graduate School of Medicine, Kyoto University, 54 Shogoin Kawahara-cho, Sakyo-ku, Kyoto 606-8507, Japan. E-mail address: kadowaki@kuhp.kyoto-u.ac.jp

The online version of this article contains supplemental material.

Abbreviations used in this article: ALDH, aldehyde dehydrogenase; ALDH1A2, aldehyde dehydrogenase 1 family, member A2; cDC, conventional dendritic cell; CLA, cutaneous lymphocyte Ag; DC, dendritic cell; DEAB, diethylaminobenzaldehyde; GUSB, β-glucronidase; mDC, myeloid DC; MFI, mean fluorescence intensity; MLN, mesenteric lymph node; MoDC, monocyte-derived DC; pDC, plasmacytoid DC; PE-Cy5, PE-Cyanin 5; RA, all-*trans*-retinoic acid; RALDH, retinal dehydrogenase; RAR, pan-RA receptor; rh, recombinant human; Treg, regulatory T; VD_3, 1α,25-dihydroxyvitamin D_3; VDR, vitamin D receptor.

www.jimmunol.org/cgi/doi/10.4049/jimmunol.1203517

In the current study, we used human DCs from blood and MLNs, as well as DCs induced from monocytes or $CD34^+$ progenitors in vitro, and explored 1) DC subsets that express a high level of RALDH2, 2) factors that induce human DCs to express a high level of RALDH2, 3) differences between humans and mice in RA-producing DC subsets and RA-inducing factors, 4) intracellular mechanisms by which RALDH2 is induced in DCs, and 5) T cell responses induced by RA-producing DCs in an RA-dependent manner. To quantify the activity of RALDH in mouse (2, 4, 5, 7, 8, 12, 19) and human (5, 19) DCs, recent studies used the Aldefluor reagent that freely diffuses into cells and is converted to a fluorescent product by aldehyde dehydrogenase (ALDH) activity. Thus, we used this reagent in combination with quantitation of ALDH1A2 mRNA to quantify the RA-producing capacity of DCs. We found that only $CD1c^+$ mDCs are capable of expressing a high level of RALDH2 in response to 1α,25-dihydroxyvitamin D_3 (VD_3) together with GM-CSF and that the $RALDH2^{high}$ mDCs induce T cells to preferentially express gut-homing molecules and Th2 cytokines in an RA-dependent manner. This study thus reveals a previously unrecognized distinctive function of human $CD1c^+$ mDCs and an unexpected role of vitamin D, that is, induction of RA from human DCs.

Materials and Methods

Culture media

RPMI 1640 (Nacalai tesque) supplemented with 10% heat-inactivated FCS (ThermoTrace), 2 mM L-glutamine, penicillin G, streptomycin (Life Technologies), and 10 mM HEPES were used for cell culture.

Reagents

Reagents and sources were as follows: recombinant human (rh)TNF, rhIL-3, rh stem cell factor, rhFLT3 ligand (PeproTech); rhGM-CSF (sargramostim; Genzyme); R848 (InvivoGen); LPS (from *Escherichia coli* O111:B4; Sigma-Aldrich); PGE_2 (MP Biomedicals); rhIL-2 (teceleukin; Shionogi & Co.); recombinant mouse GM-CSF (Kirin Brewery); anti-human IL-4 (clone MP4-25D2; eBioscience); anti-human CD28 mAbs (BD Biosciences); LE540 (Wako); U0126 (Cayman Chemical); SB203580, SP600125 (InvivoGen); VX-745 (Tocris); JAK inhibitor I (pyridone 6; Calbiochem); and SB239063 (Enzo Life Sciences). The inhibitors were dissolved in DMSO. Immunomodulatory factors added to DCs are listed in Table I. The following reagents were used for ELISA: anti–human IFN-γ mAb (clone 2G1 as capture Ab), biotinylated anti–human IFN-γ mAb (as detection Ab) and HRP-conjugated streptavidin (Endogen), OptEIA human IL-4 and IL-10 ELISA set (BD Biosciences), human IL-5 ELISA MAX Standard set (BioLegend), and a human IL-13 CytoSets kit (BioSource International).

The following Abs were used to stain human cells and are denoted as "fluorochrome-Ag." FITC-CD45RO, CD14, CD16, CD20, β_7 integrin, and cutaneous lymphocyte Ag (CLA), Alexa Fluor 488-CD1c, PE-CD103, α_4 integrin, and CD203c, PE-Cyanin 5 (PE-Cy5)-CD4, PE-Cyanin 7-CD4, and Brilliant Violet 421-CD11c were from BioLegend; FITC-CD3 and HLA-DR, PE-CD11c and CD25, and PE-Cy5-CD11c from BD Biosciences; allophycocyanin-CD141 from Miltenyi Biotec; allophycocyanin-CCR9 (clone 248621) were from R&D Systems.

The following Abs were used to stain mouse cells and are denoted as fluorochrome-Ag. FITC-B220, PE-CD11c, and allophycocyanin-CD8 were from BD Biosciences; allophycocyanin-CD103 were from BioLegend.

Cell preparations

This study was approved by the Institutional Review Board at Graduate School of Medicine, Kyoto University, and abides by the tenets of the Declaration of Helsinki. All specimens from humans were obtained from healthy donors and patients with written informed consent. To isolate human blood DCs, total PBMCs were depleted of $CD3^+$, $CD14^+$, and $CD16^+$ cells using Dynabeads goat anti-mouse IgG (Invitrogen Dynal). Then, $CD4^+CD11c^+CD141^{-/low}lin^-$ cells ($CD1c^+$ mDCs), $CD4^+CD141^{high}lin^-$ cells ($CD141^{high}$ mDCs), and $CD4^+CD11c^-CD141^{-/low}lin^-$ cells (pDCs) were purified using FACSAria cell sorter (BD Biosciences) (Supplemental Fig. 1A). The expression of CD1c on sorted blood $CD1c^+$ mDCs, $CD141^{high}$ mDCs, and pDCs is shown in Supplemental Fig. 1B. More than 98% of sorted cells were HLA-DR positive (Supplemental Fig. 1C). $CD203c^+$ basophils were isolated by sorting. Naive $CD4^+$ T cells and resting Treg cells (20) were $CD4^{high}CD25^-CD45RO^-$ cells and $CD4^{high}CD25^+CD45RO^-$ cells, respectively. Reanalysis of the sorted cells confirmed a purity of >98%. $CD8^+$ T cells were isolated from PBMCs using CD8 MicroBeads (Miltenyi Biotec).

Human MLNs from patients with colon cancer or Crohn's disease were obtained at Kyoto University Hospital or Hyogo College of Medicine Hospital, respectively. Single-cell suspension of MLNs was obtained by digestion with 500 μg/ml collagenase IV (Wako) and DNase I (Sigma-Aldrich) for 30 min, followed by sorting $CD4^+CD11c^+CD103^+lin^-CD141^{low/int}$ ($CD103^+$ mDCs), $CD4^+CD11c^+CD103^-lin^-CD141^{low/int}$ ($CD103^-$ mDCs), and $CD4^+CD11c^-CD103^-lin^-CD141^{low/int}$ (pDCs) as sorting strategy for blood DCs (Supplemental Fig. 1D). More than 99% of sorted cells were HLA-DR positive (Supplemental Fig. 1E).

Mouse $CD8^+$ and $CD8^-$ splenic DCs were prepared from BALB/c mice as described previously (Supplemental Fig. 1F) (21).

Single-cell suspensions from BALB/c mouse MLNs were prepared by collagenase (Boehringer-Ingerheim) digestion. Low-density cells were separated with BSA gradient centrifugation (Sigma-Aldrich), stained with PE-conjugated anti-CD11c, FITC-conjugated anti-B220, and allophycocyanin-conjugated anti-CD103 mAbs. DCs were first positively enriched using anti-PE microbeads (Mitenyi Biotec), and then, $CD103^+CD11c^+B220^-$ cells and $CD103^-CD11c^+B220^-$ cells were isolated as $CD103^+$ cDCs and $CD103^-$ cDCs, respectively (Supplemental Fig. 1G).

Cell culture

Human blood $CD1c^+$ mDCs, $CD141^{high}$ mDCs, and monocytes were cultured with 800 U/ml GM-CSF for 2 d. Blood pDCs were cultured with 10 ng/ml IL-3 for 2 d. Human mDCs and mouse cDCs from MLNs were cultured with 800 U/ml GM-CSF for 24 h. Human MLN pDCs were cultured with 10 ng/ml IL-3 for 24 h. Mouse splenic cDCs were cultured with 800 U/ml GM-CSF for 24 h. During these cultures, soluble factors (reagents in Table I, TLR ligands, TNF, PGE_2, LE540, or pharmacological inhibitors) were added as indicated. Concentrations of the reagents other than those listed on Table I were 10 μg/ml R848, 1 μg/ml LPS, 100 ng/ml Pam_3CSK_4, 10 ng/ml TNF, 1 μg/ml PGE_2, 1 μM LE540, 20 μM SB203580, 10 μM SP600125, and 20 μM U0126. LE540 and the pharmacological inhibitors were added to the cultures 30 min before adding other reagents. To quantify cell viability, the percentages of propidium iodide–negative cells were measured by flow cytometry after cell debris was excluded by appropriate forward scatter thresholds.

Generation of DCs from monocytes and $CD34^+$ progenitor cells

Monocytes were purified from PBMCs using CD14 MicroBeads (Miltenyi Biotec) and cultured with 800 U/ml GM-CSF and 500 U/ml IL-4 for 7 d to induce immature monocyte-derived DCs (MoDCs). LPS (100 ng/ml) was added during the last 2 d to induce maturation. Immunomodulatory factors (Table I) were added during the whole culture periods. To generate umbilical cord blood $CD34^+$ progenitor cell–derived DCs, $CD34^+$ cells were isolated using CD34 MicroBeads (Miltenyi Biotec) from cord blood and were cultured with 20 ng/ml stem cell factor, 50 ng/ml FLT3 ligand, 800 U/ml GM-CSF, and 2.5 ng/ml TNF for 7 d. Then, the cells were cultured in the absence or presence of RA, VD_3, or LPS (1 μg/ml) for 2 d.

Aldefluor assays and analysis of surface molecules

ALDH activity was determined using the Aldefluor staining kit (StemCell Technology) according to the manufacturer's protocol. Diethylaminobenzaldehyde (DEAB) (Wako) was used as an ALDH inhibitor. T cells cocultured with DCs were stained with mAbs for α_4 integrin, β_7 integrin, CLA, or CCR9. Live cells gated as propidium iodide–negative cells were acquired by FACSCalibur (BD Biosciences). Data were analyzed with FlowJo (Tree Star).

Reverse transcription and real-time PCR

$CD1c^+$ mDCs, $CD141^{high}$ mDCs, and pDCs were cultured with indicated stimuli for 24 h. Total RNA was isolated using Homogenizer and the PureLink RNA Micro Kit (Invitrogen). First-strand cDNA synthesis was performed with the ReverTra Ace qPCR RT Kit (Toyobo). Real-time PCR was performed on the Thermal Cycler Dice Real-Time System (TaKaRa). ALDH1A1, ALDH1A2, ALDH1A3, CYP27B1, vitamin D receptor (VDR), and β-glucuronidase (GUSB) were detected using TaqMan Gene Expression Assays (Applied Biosystems) and THUNDERBIRD Probe qPCR Mix (Toyobo). Primer and probe sets were as follows: *ALDH1A1*, Hs00946916_m1; *ALDH1A2*, Hs00180254_m1; *ALDH1A3*, Hs00167476_m1; *CYP27B1*, Hs00168017_m1; *VDR*, Hs01045840_m1; and *GUSB*, Hs00930627_m1.

The mRNA expression levels of each gene were normalized to those of *GUSB*.

T cell cultures with DCs

After extensive wash, $CD1c^+$ mDCs (1×10^4 cells) cultured with GM-CSF, RA, or VD_3 for 2 d were cocultured with allogeneic naive $CD4^+$ T cells or total $CD8^+$ T cells (1×10^5 cells) in the absence or presence of 1 μM LE540, 10 μg/ml rat IgG1, or 10 μg/ml anti–IL-4 mAb in 96-well U-bottom plates for 6 d. IL-2 (10 U/ml) was added to $CD8^+$ T cell culture. The $CD4^+$ T cells were restimulated at 1×10^6 cells/ml with plate-bound anti-CD3 (OKT3) and 1 μg/ml soluble anti-CD28 mAbs in 96-well flat-bottom plates for 24 h. The supernatants were analyzed for cytokines by ELISA.

Statistical analysis

Data are presented as the mean ± SE. Statistical comparisons were performed using paired two-tailed *t* test. Difference with $p < 0.05$ was considered significant.

Results

Human blood $CD1c^+$ mDCs, but not $CD141^{high}$ mDCs, express a high level of RALDH2 in response to GM-CSF and VD_3

In search of human DCs that express a high level of RALDH enzymes, different subsets of blood DCs were treated with various factors that have been reported to modulate immunostimulatory activity of DCs (Table I), and ALDH activity was measured with Aldefluor (2, 4, 5, 7, 8, 12, 19). To keep mDCs alive, we added GM-CSF (22) to $CD1c^+$ mDCs. GM-CSF by itself induced little ALDH activity (Fig. 1A, 1B). Adding RA with GM-CSF only slightly induced the activity, whereas VD_3, which modulates immunostimulatory properties of human mDCs and MoDCs (23–25), together with GM-CSF strongly upregulated the ALDH activity in $CD1c^+$ mDCs. RA plus VD_3 further augmented it (Fig. 1A, 1B). RA and VD_3 without GM-CSF induced little ALDH activity (Fig. 1A), indicating that GM-CSF is necessary for the induction. Ligands for TLRs (R848, LPS, and Pam_3CSK_4) and TNF strongly suppressed the ALDH activity, but PGE_2, which has been reported to suppress the ALDH activity in mouse bone marrow DCs (19), did not (Fig. 1C). There were no substantial differences in cell viability between different culture conditions at the time of harvest (data not shown). None of the other immunomodulatory factors (Table I) upregulated the ALDH activity in combination with GM-CSF (Supplemental Fig. 2).

In contrast to $CD1c^+$ mDCs, $CD141^{high}$ mDCs (Fig. 1D), pDCs (Fig. 1E), and CD34-derived DCs (Fig. 1F) cultured with RA and VD_3 exhibited little ALDH activity. RA and VD_3 without or with LPS slightly induced ALDH activity in MoDCs but at far lower levels than that in $CD1c^+$ mDCs (Fig. 1G). Consistent with a previous observation that human basophils express RALDH2 in response to IL-3 (26), IL-3 alone induced ALDH activity in basophils, but there was no augmentation with RA and VD_3 (Fig. 1H). There were no substantial differences in cell viability between different culture conditions (data not shown). Again, none of the other factors (Table I) upregulated the ALDH activity in combination with GM-CSF ($CD141^{high}$ mDCs, MoDCs) or IL-3 (pDCs) (Supplemental Fig. 2).

Table I. Immunomodulatory factors added to DCs

Name	Concentrations	Sources
RA	10 nM	Wako
VD_3	10 nM	Wako
IFN-α	1000 U/ml	Intron A, Schering-Plough
IL-4	500 U/ml	PeproTech
TGF-β	10 ng/ml	PeproTech
Vasoactive intestinal peptide	100 nM	LKT Laboratories
Rosiglitazone	10 μM	Alexis Biochemicals
T0901317	1 μM	Cayman Chemicals
Rapamycin	100 ng/ml	PeproTech
Tacrolimus	100 ng/ml	Enzo Life Sciences
Cyclosporin A	1000 ng/ml	Sigma-Aldrich
Dexamethasone	1 μM	Sigma-Aldrich

We also cultured monocytes with GM-CSF in the absence or presence of the immunomodulatory factors (Table I). RA plus VD_3 substantially induced ALDH activity, albeit to a lesser extent than that in $CD1c^+$ mDCs. None of the other factors substantially induced the activity (Supplemental Fig. 2).

We next examined whether the ALDH activity detected by Aldefluor correlates with the expression levels of mRNA for *ALDH1A2* (encoding RALDH2) in $CD1c^+$ mDCs, $CD141^{high}$ mDCs, and pDCs. Consistent with the results by Aldefluor analyses, GM-CSF alone induced little expression of ALDH1A2 mRNA in $CD1c^+$ mDCs, and the addition of VD_3 markedly upregulated it (Fig. 1I). The addition of RA to GM-CSF and to GM-CSF plus VD_3 slightly increased the expression of ALDH1A2 mRNA, but R848 completely suppressed it. There was almost no expression of ALDH1A2 mRNA in $CD141^{high}$ mDCs or pDCs. mRNAs for *ALDH1A1* and *ALDH1A3* (encoding RALDH1 and RALDH3) were hardly expressed in $CD1c^+$ mDCs even in the presence of the indicated stimulation (Fig. 1J, 1K).

Collectively, 1) $CD1c^+$ mDCs, but not the other human blood DC subsets, express a high level of RALDH2 in response to GM-CSF plus VD_3, and exogenous RA augments the expression, and 2) proinflammatory factors (TLR ligands and TNF) suppress the expression of RALDH2.

Human $CD103^-$ mDCs in MLNs gain ALDH activity in response to the VD_3-containing stimulus

To examine whether human MLN DCs exhibit ALDH activity as mouse MLN $CD103^+$ DCs do (3, 4), DC subsets were isolated from MLNs of patients with colon cancer or Crohn's disease in the same way as done for blood DCs (Supplemental Fig. 1D). Unlike in blood, $CD141^{high}$ mDCs were not identified as a discrete population in MLNs. $CD11c^{high}$ mDCs were subdivided into $CD103^+$ and $CD103^-$ mDCs. pDCs did not express CD103.

Unlike mouse MLN DCs, freshly isolated human $CD103^+$ MLN mDCs did not have ALDH activity (Fig. 2). Unexpectedly, $CD103^-$ but not $CD103^+$ MLN mDCs gained a high level of ALDH activity in response to GM-CSF, RA, and VD_3. pDCs did not exhibit ALDH activity. All the above results were the same in DCs from both colon cancer and Crohn's disease. Thus, in humans, $CD103^-$ but not $CD103^+$ MLN mDCs may be RA-producing DCs in situ in the intestine.

Mouse splenic and MLN cDCs gain ALDH activity in response to GM-CSF alone

Genome-wide expression profiling clustered human $CD141^{high}$ mDCs and $CD1c^+$ mDCs with mouse $CD8^+$ cDCs and $CD8^-$ cDCs, respectively (18). Thus, we examined whether VD_3 differentially induces mouse splenic cDC subsets to gain ALDH activity. As we reported (4), GM-CSF alone was sufficient to induce high levels of ALDH activity in both $CD8^+$ DCs and $CD8^-$ DCs in the spleen (Fig. 3A). Neither RA nor VD_3 augmented the activity. Unlike in human $CD1c^+$ mDCs, LPS did not suppress it. There were no substantial differences in cell viability between different culture conditions (data not shown). We also examined ALDH activity in mouse MLN cDCs in the absence or presence of the VD_3-containing stimulus. As reported (3), fresh $CD103^+$ but not $CD103^-$ cDCs in MLNs exhibited ALDH activity (Fig. 3B). Again, GM-CSF alone was sufficient to induce high levels of ALDH activity in both $CD103^+$ and $CD103^-$ cDCs, and the addition of RA and VD_3 did not augment it.

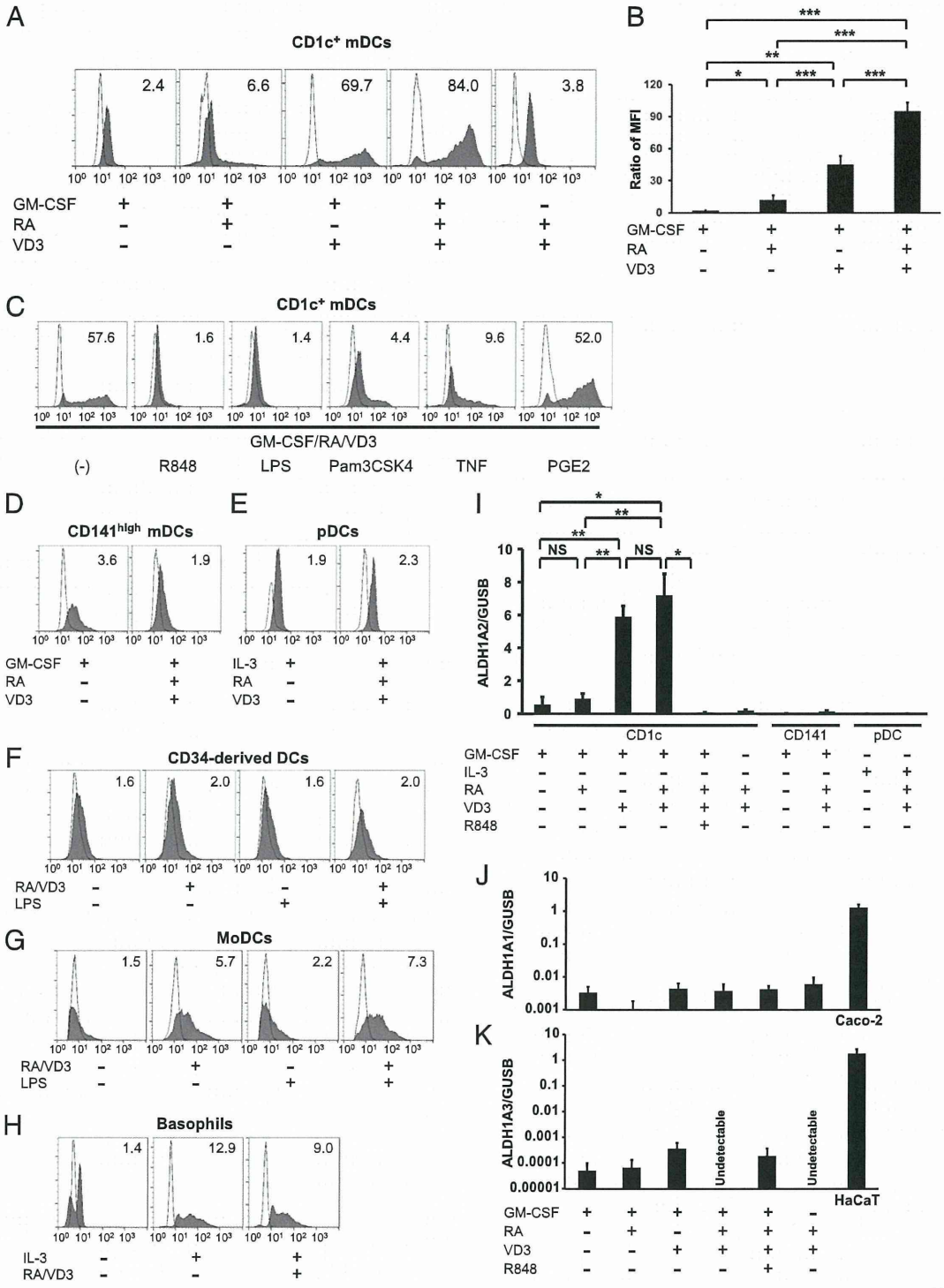

FIGURE 1. ALDH activity and ALDH1A2 mRNA expression in human blood DC subsets and basophils. CD1c$^+$ mDCs (**A–C**), CD141^{high} mDCs (**D**), pDCs (**E**), and basophils (**H**) were cultured in the absence or presence of the indicated reagents for 2 d. CD34$^+$ progenitor cell–derived dendritic cells (CD34-derived DCs) (**F**) and MoDCs (**G**) were cultured as indicated in *Materials and Methods*. The cells were incubated with Aldefluor in the absence (solid histograms) or presence (open histograms) of an ALDH inhibitor DEAB and were analyzed by flow cytometry. The numbers shown with each histogram represent ratios of mean fluorescence intensity of Aldefluor in the absence of DEAB to that in the presence of DEAB. (**I**) ALDH1A2 mRNA expression was measured by real-time RT-PCR. CD1c$^+$ mDCs, CD141^{high} mDCs, and pDCs were cultured with the indicated stimuli for 24 h. The expression levels were normalized to those of GUSB. $*p < 0.05$, $**p < 0.01$, $***p < 0.001$. ALDH1A1 (**J**) and ALDH1A3 (**K**) mRNA expressions were measured by real-time RT-PCR. CD1c$^+$ mDCs were cultured with the indicated stimuli for 24 h. Human colon cancer cell line Caco-2 and human keratinocyte cell line HaCaT were used as positive controls for ALDH1A1 and ALDH1A3, respectively. The expression levels were normalized to those of GUSB. Note the low levels of the scales. The data are representative of three (A, D–G) or two (H) independent experiments and are shown as the mean ± SE of 8 (B), 4 (I), or 3 (J, K) independent experiments.

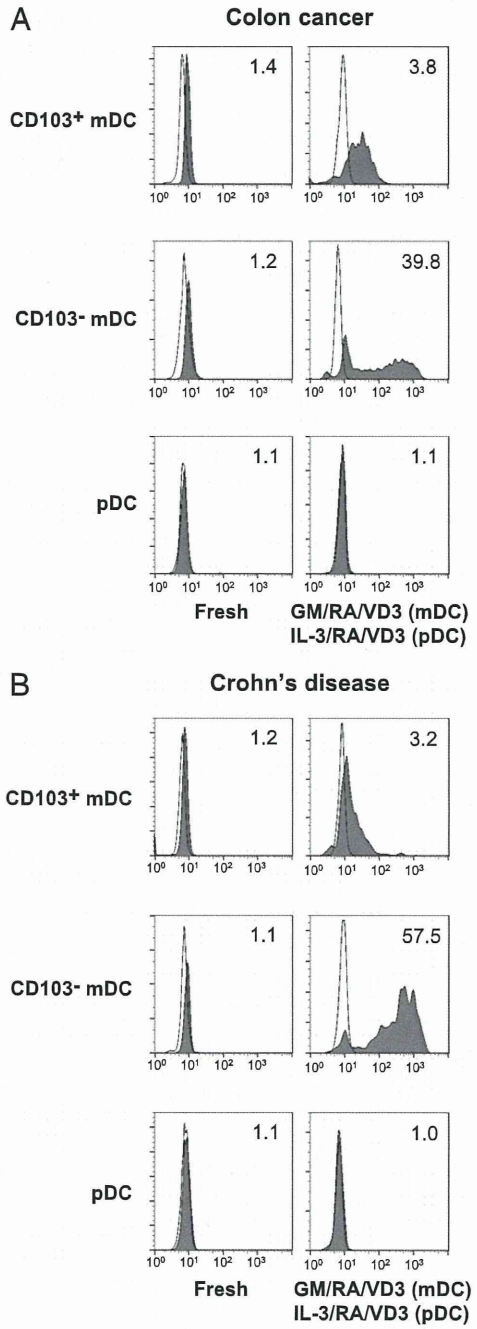

FIGURE 2. ALDH activity in human MLN DC subsets. $CD103^+$ mDCs, $CD103^-$ mDCs, or pDCs were purified from MLNs of patients with colon cancer (**A**) or Crohn's disease (**B**) and were analyzed without culture or after culture with the indicated stimuli for 24 h. Histograms and the numbers shown with them are presented as in Fig. 1. The data are representative of three (A) or two (B) independent experiments.

Collectively, the RA-producing DC subsets and the stimulation to induce RA production are different between human and mouse DCs, in that 1) both of the cDC subsets in mouse spleen ($CD8^+$ and $CD8^-$) and MLNs ($CD103^+$ and $CD103^-$) exhibit ALDH activity in response to GM-CSF alone, 2) VD_3 does not induce or increase the activity, and 3) TLR signaling does not suppress the activity in mice.

Engagement of RA receptor is necessary for the high level of RALDH2 expression induced by VD_3

We investigated the mechanisms by which GM-CSF, RA, and VD_3 induce a high level of RALDH2 in human $CD1c^+$ mDCs. Exogenous RA augmented the expression of RALDH2 induced by VD_3 (Fig. 1A, 1B). Thus, we examined whether endogenous RA is responsible for the induction of RALDH2 by VD_3. A pan-RA receptor (RAR) antagonist LE540 diminished the induction of ALDH activity by VD_3 (Fig. 4A), indicating that endogenous RA or possibly RAR agonists contained in the serum are necessary for the induction of a high level of RALDH2 by VD_3. However, the induction of RALDH2 by RA alone was much weaker than the induction by VD_3 (Fig. 1A, 1B), indicating that combined signals by RA and VD_3 are necessary for the full expression of RALDH2.

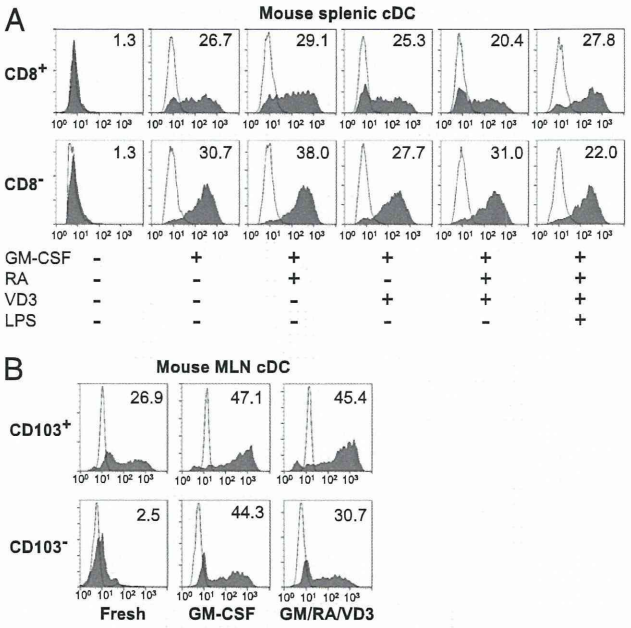

FIGURE 3. ALDH activity in mouse splenic and MLN cDC subsets. (**A**) $CD8^+$ and $CD8^-$ mouse splenic cDCs were cultured without or with the indicated stimuli for 24 h. (**B**) $CD103^+$ and $CD103^-$ mouse MLN cDCs were analyzed without culture or were cultured with the indicated stimuli for 24 h. Histograms and the numbers shown with them are presented as in Fig. 1. The data are representative of three independent experiments.

When cultured with GM-CSF, RA, and VD_3, $CD1c^+$ mDCs expressed only a low level of mRNA for CYP27B1, the enzyme that converts 25-hydroxyvitamin D_3 into its bioactive form VD_3 (27), although $CD1c^+$ mDCs expressed a high level of CYP27B1 mRNA in the presence of R848 (Supplemental Fig. 3A). Thus, endogenous VD_3 does not appear to participate in the induction of RALDH2.

$CD1c^+$ mDCs, $CD141^{high}$ mDCs, and pDCs expressed similar levels of mRNA for the nuclear VDR, consistent with a previous report (Supplemental Fig. 3B) (25). Thus, the marked effect of VD_3 on the induction of RALDH2 in $CD1c^+$ mDCs is not likely to be determined by differential expression of VDR among the DC subsets, but $CD1c^+$ mDCs may have distinctive molecular machineries to express RALDH2 in response to VD_3.

Activation of p38 is necessary for the induction of RALDH2

We investigated signaling pathways involved in the induction of RALDH2 in $CD1c^+$ mDCs. After stimulation with GM-CSF, RA, and VD_3, the DCs started to express ALDH1A2 mRNA at 6 h, and the expression reached its peak at 24 h (Fig. 4B). This slow kinetics indicates that the induction of ALDH1A2 mRNA is not due to direct transcriptional activity of VDR. Instead, secondary signals downstream of VDR and RAR are likely to mediate the induction of ALDH1A2 mRNA.

A pan-JAK inhibitor strongly blocked the induction of ALDH activity (Fig. 4C) in accord with the dependence of the induction

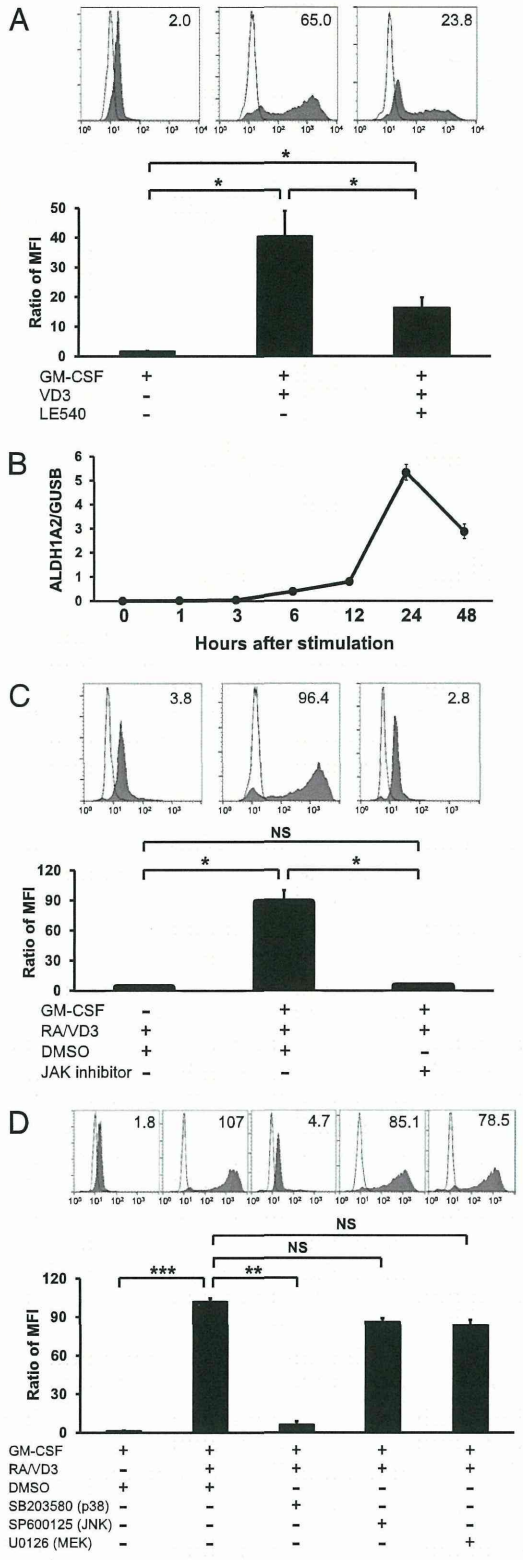

FIGURE 4. The induction of ALDH activity in CD1c$^+$ mDCs is dependent on RAR, JAK, and p38 signaling. (**A**, **C**, and **D**) CD1c$^+$ mDCs were cultured with the indicated reagents for 2 d. Histograms and the numbers shown with them are presented as in Fig. 1. The histograms are representative data, and the graphs show the mean ± SE of four (A) or three (C, D) independent experiments. (**B**) CD1c$^+$ mDCs were cultured with GM-CSF, RA, and VD_3 for the indicated time periods. ALDH1A2 mRNA expressions were measured by real-time RT-PCR. The expression levels were normalized to those of GUSB. The data are presented as the mean ± SD of duplicate samples in one of two independent experiments.

on GM-CSF. Three p38 MAPK inhibitors, SB203580 (Fig. 4D), SB239063 (28), and VX-745 (29) (data not shown), also blocked the induction. In contrast, inhibitors against JNK (SP600125) or MEK 1/2 (U0126) did not do so (Fig. 4D). There were no substantial differences in cell viability between different culture conditions (data not shown). Thus, RALDH2 in CD1c$^+$ mDCs is induced in a p38-dependent manner.

RALDH2^{high} mDCs induce T cells to acquire gut-homing capacities in an RA-dependent manner

RA derived from mouse intestinal DCs endows T cells with the expression of gut-homing molecules, $\alpha_4\beta_7$ integrin and CCR9 (1). Furthermore, intestinal DCs reciprocally suppress the expression of skin-homing molecules, P- and L-selectin ligands, on T cells (30). Thus, we examined homing properties of T cells stimulated with GM-CSF/RA/VD_3–treated RALDH2^{high}CD1c$^+$ mDCs (hereafter referred to as RALDH2^{high} mDCs). Naive CD4$^+$ T cells stimulated with allogeneic RALDH2^{high} mDCs expressed a higher level of $\alpha_4\beta_7$ integrin (Fig. 5A, 5B) and reciprocally a lower level of a P- and L-selectin ligand CLA (Fig. 5C) than T cells stimulated with GM-CSF–treated RALDH2^{low}CD1c$^+$ mDCs (hereafter referred to as RALDH2^{low} mDCs). The upregulation of $\alpha_4\beta_7$ integrin and downregulation of CLA by RALDH2^{high} mDCs were abrogated by LE540. These data indicate that RALDH2^{high} mDCs induce gut-homing and reduce skin-homing properties of T cells in an RA-dependent manner. RALDH2^{high} mDCs did not induce allogeneic naive CD4$^+$ T cells or total CD8$^+$ T cells to express a detectable level of CCR9 (data not shown).

RALDH2^{high} mDCs induce naive CD4$^+$ T cells to acquire Th2 cytokine–producing capacities in an RA-dependent manner

We examined cytokine-producing properties of naive CD4$^+$ T cells stimulated with allogeneic mDCs. CD4$^+$ T cells stimulated with RALDH2^{high} mDCs secreted significantly higher levels of Th2 cytokines IL-4, IL-5, and IL-13 than those stimulated with RALDH2^{low} mDCs (Fig. 6A). This effect was abrogated by LE540 (Fig. 6A), but not by anti–IL-4 neutralizing mAb (Fig. 6B). CD4$^+$ T cells stimulated with RALDH2^{high} mDCs secreted a similar level of IFN-γ, compared with those stimulated with RALDH2^{low} mDCs (Fig. 6C). CD4$^+$ T cells stimulated with RALDH2^{high} mDCs secreted a significantly higher level of IL-10 than those stimulated with RALDH2^{low} mDCs, but the induction of IL-10 was not abrogated by LE540 (Fig. 6C). These data indicate that RALDH2^{high} mDCs induce naive CD4$^+$ T cells to acquire the ability to produce high levels of Th2 cytokines in an RA-dependent and IL-4–independent manner.

We also examined whether naive CD4$^+$ T cells stimulated with RALDH2^{high} mDCs acquire regulatory activity. Although CD4$^+$ T cells stimulated with RALDH2^{high} mDCs slightly suppressed proliferation of concomitant T cells, the effect was much weaker than that exhibited by resting Treg cells directly purified from blood (20) (data not shown). Thus, RALDH2^{high} mDCs do not have an unambiguous regulatory T cell–inducing ability detectable by our assay.

Discussion

RA plays a critical role in maintaining immune homeostasis in the intestine (27). Human DCs that produce a high level of RA remained unknown. The present study identifies blood CD1c$^+$ mDCs as a DC subset that potently produces RA in response to VD_3 in humans. RALDH2^{high} CD1c$^+$ mDCs induced T cells to preferentially express gut-homing molecules and Th2 cytokines in an RA-dependent manner. This study reveals a novel component in